Prediction of Ideal Wind Turbine Blade Angle and Size for Minimum Electricity Cost Using CFD and Actual Wind Records

Munir A. Elfarra*‡, Salem Silini**, Shawkat S. Gasaymeh*

*Department of Aircraft Maintenance Technology, Abu Dhabi Polytechnic, Abu Dhabi, UAE

**High Institute of Science and Technology, Tripoli, Libya

(munir.elfarra@actvet.gov.ae, salemomer19@gmail.com, shawkat.gasaymeh@actvet.gov.ae)

‡Corresponding Author; Munir Elfarra, Abu Dhabi Polytechnic, Al Ain Campus, Al Ain, UAE, Tel: +971569398580, munir.elfarra@actvet.gov.ae

Received: 09.11.2023 Accepted:01.02.2024

Abstract- The research merges studies on the computational fluid dynamics of wind turbine blades with evaluations of actual wind data. We took the stall regulated NREL VI wind turbine, as our reference. Through the CFD approach, we identified the ideal pitch angle at the blade tip that amplifies power output (ensuring the rated power isn't surpassed) for wind velocities ranging between 5-20 m/s, thereby transitioning the turbine from stall-regulated to pitch-regulated. The ideally pitched blade was scaled up by three varying factors: 1.05, 1.1, and 1.15. We then determined the power curves for each scale using CFD.

For two different locations, we assessed the wind to predict yearly energy output and to compute electricity costs. This evaluation used actual wind records from these sites and our derived power curves. The assessment employed the well-known maximum likelihood technique, which operates on Weibull distribution based on two parameters. The wind assessment includes the calculation of the annual energy production, which is based on the computed power curves using CFD, and the present value of costs. The PVC is used to calculate the price at which the generated electricity should be sold so that the project investment cost is redeemed. Our findings indicated a noteworthy increase in yearly energy yield and a marked reduction in electricity generation costs.

Keywords Wind energy, CFD, pitch angle, annual energy production, electricity cost, blade sizing.

1. Introduction

Considered to be is one of the most competitive and cost-effective renewable energy sources, wind energy is expected to keep growing rapidly in the coming years. One of the most crucial issues of wind energy is the price at which the generated electricity is to be sold to make the energy project more feasible within the wind turbine life time. The lower the price of the generated electricity, the more feasible the project is and the less the investment risks are. Aerodynamic shape design and optimization of the turbine blades are performed to increase their performance in generating energy and hence decreasing the electricity cost. Most of the problems related to aerodynamic design and optimization are conducted using blade element momentum theory (BEM) approaches [1] due to their simplicity and less computational time [2]. Conversely, CFD based methods are more complicated and require more computational time but they are able to determine the whole flow characteristics and accurately capture the 3-D, compressibility, rotational and viscous effects unlike the BEM methods. CFD methods for analyzing, designing and optimizing blades of wind turbines have been increasingly used in literature [3].

Dhert et al. [2] have developed shape optimization a framework using 3-D Reynolds-averaged Navier-Stokes (RANS) solver and an optimization algorithm. The aim was to increase the torque coefficient. The airfoil shape, pitch angle and twist distribution were considered as the design variables. The main outcome of their work was to increase the torque coefficient by 22%.

Elfarra et al. [4] have optimized the shape of a wind turbine blade winglet using 3-D RANS CFD. Their results showed a 9% increase in power production. The same authors

have investigated different tip configurations for NREL VI wind turbine blades in [5] and they have attained an improvement in the power output.

In [6], Economon et al. implemented a RANS solver incorporating continuous adjoint method in order to find the optimum shape of the NREL VI blade. Their results demonstrated an increase of 4% in the torque which was the objective function.

Alaimo et al. [7] have estimated the performance of a slotted blade Savonius wind turbine for different slot positions using CFD. Their results have shown that improving the rotor performance is possible by altering the slot positions. Other studies on vertical axis wind turbines using CFD have been conducted in [8, 9].

Cao et al. [10] have coupled an actuator disk (AD) model with a RANS solver in order to optimize a wind turbine rotor blade. They have used the blade chord, twist and thickness as design variables. Their results have shown that the optimization framework they have developed can be used for enhancing the rotor aerodynamic performance. A similar study by Cao et al. [11] was conducted to see the effect of wake in the optimization framework. In their study, the rotational speed was included as a design variable besides the shape parameters.

The power output results obtained from CFD analysis are used to predict the annual energy production (AEP) and hence the electricity cost. However, to predict the AEP, wind data are also needed besides the turbine power output. Indeed, prior to setting up a wind farm, it's essential to thoroughly examine the site's wind statistics and capacity to reduce financial uncertainties [12]. Among various techniques to assess wind energy capability, the Weibull function approach, rooted in probability density functions (PDF), is the most frequently employed one.

The current research combines CFD analysis of a prototype wind turbine to determine its power curve with an evaluation of actual wind data. The study is subdivided into three main parts. Firstly, using CFD methods, the optimum blade tip pitch angle (or just pitch angle for simplicity) for maximizing the power output for different wind speeds is obtained and the turbine power curve of the optimum pitch is computed. Secondly, the wind turbine blades are enlarged by different scale factors and new power curves are obtained for each scale factor using CFD methods and at the optimum pitch angles computed previously. Finally, wind energy assessment for two sites is conducted using CFD results of the optimum pitch and the scales. The wind assessment includes the calculation of the AEP, which is based on the computed power curves using CFD, and the present value of costs (PVC). The PVC is used to calculate the price at which the generated electricity should be sold so that the project investment cost is redeemed. The impacts of both the optimum pitch and sizing on the AEP and PVC are discussed.

The model wind turbine selected for this research is the NREL VI turbine blade and the wind data are obtained from Almqrun and Tarhuna sites which are located in Libya.

2. Wind Turbine and Validation of CFD Results

2.1. Model Wind Turbine

The model wind turbine used in the current study is the NREL Phase VI - sequence H wind turbine [13, 14]. The blades of this turbine are twisted and tapered. For more information, the reader might refer to [13] and [14].

2.2. Flow Solver and Boundary Conditions

In the present analysis, all calculations are performed with the FINE/Turbo CFD software. This solver operates in three dimensions and is suitable for compressible, structured, multi-block, finite volume computations. To handle incompressible flow calculations, the solver incorporates the Hakimi preconditioning for low Mach numbers, as referenced in source [15]. The solver approaches the steady state Reynolds-Averaged Navier-Stokes (RANS) Equations. The Shear-Stress Transport (SST) turbulence model is used for the turbulence components.

The evaluation of the flowfield utilizes three distinct boundary conditions: farfield, solid and periodic conditions. The solid boundary conditions assume an adiabatic wall with a no-slip situation, setting the fluid velocity at the wall to match that of the blade. The farfield flow variables are determined using Riemann invariants which take into account the ambient temperature, pressure, and velocity, with freestream parameters sourced from experimental findings noted in references [13, 14].

2.3. Mesh

An O4H grid topology structured mesh enveloping the blades has been produced using AutoGrid5 program. The mesh generation was tailored for an individual blade, with periodic boundary conditions applied to simulate the effects of adjacent blades. The complete mesh, encompassing both the blade surface and the surrounding flow, consists of approximately 7 million points. To achieve a y+ value near 1, the initial cell layer thickness nearest to the blade wall was established at 3x10-6 meters. The baseline blade's mesh configuration is depicted in Figure 1.

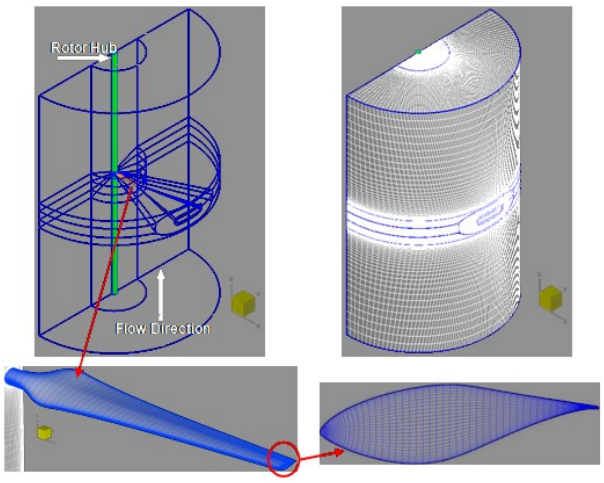


Fig. 1. The mesh.

The computational results obtained from the software were validated against experimental data in terms of power. production and spanwise pressure coefficient distributions in previous works [4, 5].

3. Optimum Blade Pitch Angle

The fundamental wind turbine in this study operates on a stall regulation mechanism, which keeps the pitch angle static regardless of variations in wind velocity. When the wind velocity exceeds a certain threshold, intense vortices are produced blade wake, leading to a stall condition. This results in a diminished power output beyond the turbine's rated speed, which is illustrated in Figure 2. The research aims to identify an optimal pitch angle that yields the maximum power output at various speeds without exceeding the turbine's rated power capacity. Should the potential maximum power exceed the rated limit, the pitch angle that aligns with the rated power is then considered optimal. This method effectively converts the turbine from stall to pitch regulated for managing power output. For wind speeds lower than the rated level, the optimal pitch angle is determined to enhance power production at those lower velocities.

To ascertain the ideal pitch angles, a series of CFD simulations were conducted for different wind speeds, adjusting pitch angles accordingly. The findings, which are graphically represented in Figure 3, reveal that for each speed up to 14 m/s, the power output initially rises with an increase in pitch angle until it reaches a peak, after which it begins to decline.

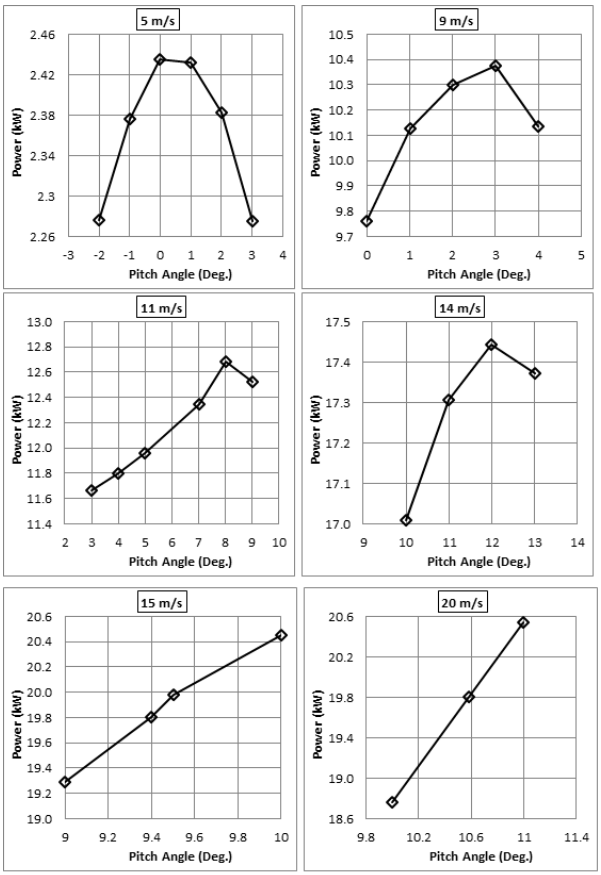


Fig. 2. Optimum blade pitch angle versus wind speeds.

The pitch angle that coincides with the peak power output is therefore designated as the optimal pitch angle for that particular wind speed. At a speed of 15 m/s, the wind turbine generates its rated power output of around 20 kW at an angle of 9.4 degrees, indicating that 15 m/s represents the rated speed and 9.4 degrees is the optimal pitch angle for this speed. Table 1 summarizes the best pitch angles and the corresponding rise in power generation across different wind velocities. Notably, at 9 m/s, the optimal pitch is identical to the baseline pitch angle. Figure 3 offers a comparative view of the power output using optimum pitch angles against the baseline power of the turbine, highlighting an average power increase of about 80% across the spectrum of wind speeds.

4. Sizing of a Wind Turbine Blade

Wind farms with below-average wind speeds can benefit from installing turbines with larger blades to harness more wind energy, thus increasing electricity production. Part of this research investigates the impact of the size of a wind turbine blade on the produced energy to establish a correlation between blade size and output power.

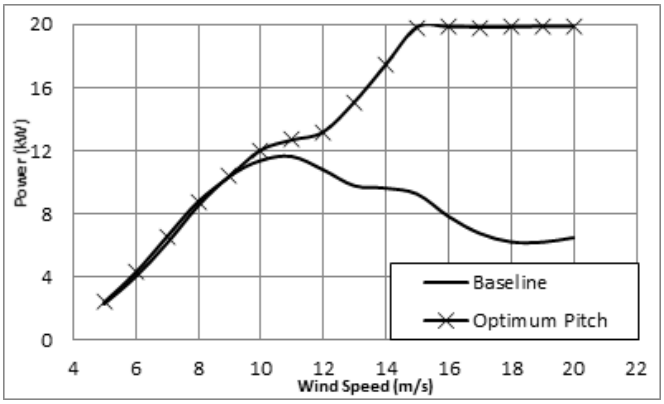


Fig. 3. Optimum pitch power vs the baseline pitch power.

Table 1. Optimum pitch angles at various wind velocities

Wind Speed (m/s)	Optimum Pitch Angle (deg.)	Percentage of Increase in Power Output (%)
5.0	0.0	6.89
6.0	0.0	7.69
7.0	0.0	7.13
8.0	0.0	3.28
9.0	3.0	0.00
10.0	4.0	5.59
11.0	8.0	10.00
12.0	8.0	21.90
13.0	10.0	53.91
14.0	12.0	80.78
15.0	9.4	113.33
16.0	9.9	152.02
17.0	9.6	192.21
18.0	9.9	217.81
19.0	10.2	218.70
20.0	10.6	204.65

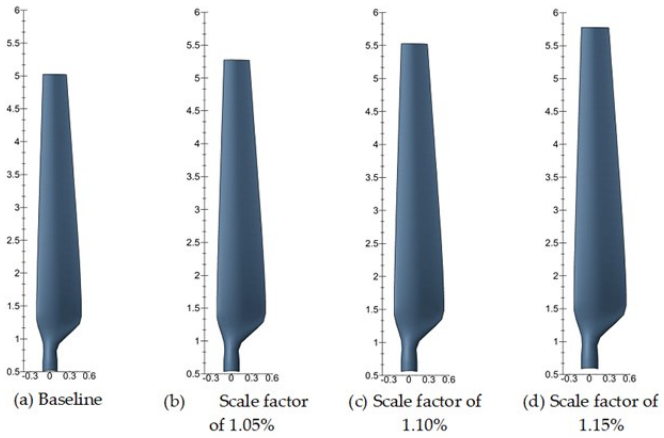


Fig. 4. Blade sizing with different scales.

Table 2. RPM change with scale factor

Scale Factor	RPM
Baseline	72
5 %	68.58
10 %	65.46
15 %	62.61

Analysis was conducted on three differently sized blades, each scaled up from the baseline blade by increments of 5%, 10%, and 15%. The outcomes of this comparative analysis are depicted in Figure 4.

Two specific conditions were maintained during the scale-up process. Firstly, the tip speed of the blades was kept consistent with that of the baseline blade by reducing the revolutions per minute (RPM) such that the increased blade size would not alter the tip speed. The relationship between RPM and the scale factor is detailed in Table 2. Secondly, to avoid surpassing the rated (nominal) power output of the baseline blade, the pitch angle for the new sized (scaled) blades was adjusted at wind speeds greater than the rated speed, ensuring that the generated power remained at or below the baseline blade's rated power.

The comparative analysis of the power curves for the scaled blades against the original blade and the optimized blade is presented in Figure 5, using the consistent CFD methodology previously outlined. It is observed that the power curves of the new scaled blades for wind speeds below the rated one were determined using the ideal pitch angles identified earlier. The 19.8 kW rated power value is fixed in the scenarios where wind speeds meet or exceed the rated speed. From Figure 5, it is apparent that the rated wind speed of the blade scaled by a factor of 1.05 remains at 15 m/s, aligning with the baseline blade's rated speed, albeit at a different pitch angle. For blades scaled by factors of 1.1 and 1.15, the rated power is achieved at reduced wind speeds of 14 m/s and 13 m/s, respectively, indicating that increasing the scale factor allows the turbine to reach its rated power at lower wind speeds.

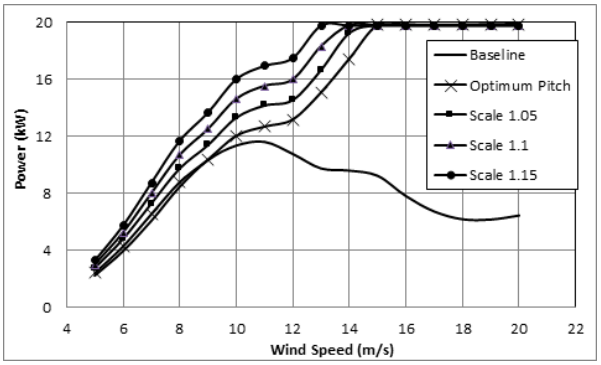


Fig. 5. Computed power curves various scales.

Table 3. Percentage increase in power output at various scales

Wind Speed (m/s)	Percentage of Increase in Power Output (%)		
	Optimum Pitch with 1.05 scale	Optimum Pitch with 1.1 scale	Optimum Pitch with 1.15 scale
5.0	12.55	23.69	35.51
6.0	11.35	22.30	33.88
7.0	10.98	22.04	33.63
8.0	10.78	21.74	33.31
9.0	9.63	20.54	31.92
10.0	10.50	21.47	33.12
11.0	10.33	21.10	32.30
12.0	10.29	21.32	32.88
13.0	10.42	21.43	-
14.0	10.37	-	-

The data in Table 3 shows a direct comparison of power output increases at different blade scales for wind speeds under the rated threshold. The findings indicate that a 5% increase in blade size, represented by a 1.05 scale factor gives a 10.7% average boost in power output. Further scale increments of 1.1 and 1.15 correspond to average power output increases of 21.7% and 33.1%, respectively. This trend suggests a potential proportional relationship where every 5 percent increase in the size could lead to an approximate 11% rise in power generation. However, to substantiate this pattern, more comprehensive research is necessary, involving a variety of wind turbines and scale factors.

The study has successfully demonstrated that optimizing the pitch angle and enlarging the blade size can significantly enhance power output. The principal aim, however, is to evaluate the impact of these optimizations on the cost of electricity generation. This assessment is based on the adjusted wind turbine power curves, site-specific wind data, and the overall cost of the wind turbine infrastructure. The subsequent section will delve into wind resource evaluation using actual wind data to further this analysis.

5. Wind Energy Assessment Methodology

5.1. Wind Data

Understanding the patterns of wind behavior in a given area is crucial for appraising and harnessing wind energy. This research undertakes an investigation of wind power potential at two coastal sites in Libya, namely Almqrun and Tarhuna.

Table 4. Average wind speed data

Site	Monthly Average Wind Speeds (m/s)												Annual Averages (m/s)
	Jan.	Feb.	Mar.	Apr.	May	Jun.	Jul.	Aug.	Sep.	Oct.	Nov.	Dec.	
Almqrun	4.47	4.59	5.29	5.47	5.28	5.08	5.22	4.70	4.62	3.76	4.09	5.06	4.81
Tarhuna	5.63	7.26	6.80	9.66	6.88	7.37	5.95	6.38	6.41	7.02	6.15	5.60	7.25

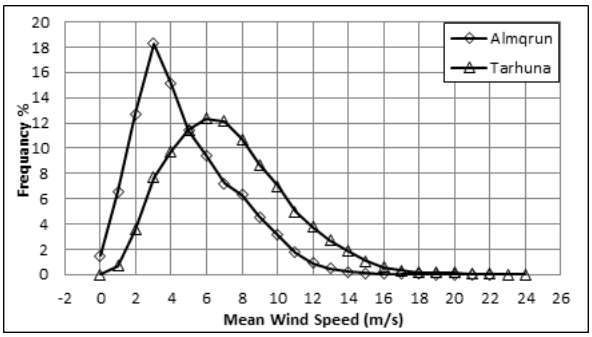


Fig. 6. Annual frequency distributions measured at 20 m.

The data related to the wind speed for this assessment were sourced from the Libyan Meteorological Authority, recorded at a height of 20 meters above ground. According to Table 4, which presents the monthly and yearly mean wind velocities for both locations, it is evident that Tarhuna experiences consistently higher average wind speeds throughout the year, in contrast to the moderately lower speeds observed in Almqrun.

Figure 6 displays the annual frequency curves of wind speed measurements for all the sites under consideration. The curves in the figure show an increase leading up to a maximum value before declining. Furthermore, the peak values of these frequency distributions vary from 12% to 18%.

5.2. Cumulative Distribution Function and Weibull Parameters

For the computation of annual energy output, knowledge of the Cumulative Distribution Function (CDF) is required. Commonly, the CDF is determined by employing the Weibull parameters: the shape factor parameter 'k' and the scale factor parameter 'c', as depicted in Eq. 1. This method has been widely adopted in the field, as referenced by numerous studies [16-18]. Other method based on cubic splines was also used in literature [19].

$$CDF(v) = 1 - exp\left[-\left(\frac{v}{c}\right)^{k}\right] \qquad \text{.....(1)}$$

$$k = \frac{\pi}{\sqrt{6}}\left[\frac{N(N-1)}{N(\sum ln^2(v_i)) - (\sum ln(v_i))^2}\right]^{0.5} \qquad \text{.....(2)}$$

$$c = \left(\frac{\sum (v_i)^k}{N}\right)^{\frac{1}{k}} \qquad \text{.....(3)}$$

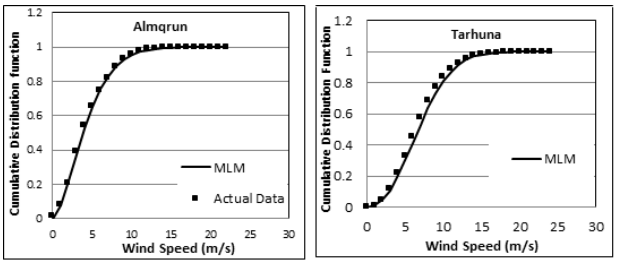


Fig. 7. Comparison of the cumulative distribution function.

Various methods exist for estimating the Weibull parameters. In this particular study, the maximum likelihood method (MLM) has been applied. MLM is a statistical approach that uses time series data of wind speeds to calculate the Weibull parameters, which is illustrated in equations 2 and 3 [20].

Using equations 2 and 3 and the wind information of the analyzed sites, the shape and scale factors are calculated as k = 2.0 and c = 5.59 for the Almqrun site and k = 2.54 and c = 8.34 for the Tarhuna site.

The results for the CDF are plotted and fitted against the actual data in Figure 7. The results show that the estimated functions fit well against the actual data.

5.3. Error Analysis

Error analysis is performed by determining the Root Mean Square Error (RMSE) to confirm the precision of the Weibull distributions derived from the maximum likelihood method. RMSE quantifies the discrepancies between the frequencies predicted by the Weibull function and the actual observed frequencies. This measure of the residuals is specified in Eq. 4 [21].

$$RMSE = \sqrt{\frac{1}{N}\sum_{i=1}^{N}(y_i - x_i)^2} \qquad \text{.....(4)}$$

In this context, 'N' represents the total count of observations (or the number of real data points), y_i, denotes the true frequency, and, x_i, signifies the frequency as predicted by the Weibull function. The RMSE values calculated using Equation 4 for Almqrun and Tarhuna are 0.0278 and 0.0109, respectively. The low magnitude of these RMSE values corroborates the reliability of the MLM in predicting wind frequencies.

5.4. Annual Energy Production (AEP)

Calculating AEP is a pivotal step in assessing wind energy projects. This involves integrating the long-term wind speeds data distribution and the power curve of a

particular wind turbine. This integration yields the energy produced at various wind speeds, culminating in the total energy output over a year. The mathematical expression for the AEP is documented and can be found in reference [22].

To estimate the likelihood that a given wind speed, v_0, will occur between two specific wind speeds, v_i and v_{i+1}, one can use the CDF as described in Eq. 5.

$$F(v_i < v_0 < v_{i+1}) = exp\left[-\left(\frac{v_i}{c}\right)^k\right] - exp\left[-\left(\frac{v_{i+1}}{c}\right)^k\right] \quad .....(5)$$

The total AEP is computed as:

$$AEP = \sum_{i=1}^{N-1} \frac{1}{2}[P(v_{i+1}) + P(v_i)] \cdot F(v_i < v_0 < v_{i+1}) \cdot 8760 \quad .....(6)$$

Here, $P(v_i)$, represents a certain wind turbine power generation at a wind speed v_i, where 8760 denotes the total number of hours in one year.

5.5. Cost Analysis

The analysis of costs is approached through the present value of costs (PVC) formula, a method referenced and utilized by many researchers [23, 24]. This formula is instrumental in estimating the cost per kilowatt-hour (kWh) of electricity produced by a wind turbine. Computation of PVC is derived from Eq. 7.

$$PVC = I + C_{omr}\left[\frac{1+i}{r-i}\right] \times \left[1 - \left[\frac{1+i}{1+r}\right]^t\right] - S\left[\frac{1+i}{1+r}\right]^t \quad .....(7)$$

Where;
t: life time of the tubine
I: Investment = turbine cost + 20% of the turbine cost
C_{omr}: Operation, Maintenance and Repair cost (OMR) = 25% of the annual cost of the turbine
i: inflation rate
r: interest rate
S: Scrap value = 10% of the investment

Following the computation of the PVC, the cost for each kilowatt-hour (kWh) of electricity generated from the turbine is determined. This cost is calculated in U.S. cents per kWh as delineated in Eq. 8.

$$kWh\ cost = \frac{PVC}{AEP \times t} \times 100 \quad .....(8)$$

6. Results and Discussion

This section details the prediction of the Annual Energy Production (AEP) and performs a cost analysis for the sites under study. It considers three scenarios: the use of the original wind turbine, the pitch wise optimum turbine and turbines of varying scales.

By integrating the power curve obtained from CFD computations for all the blade designs in question with the wind data obtained from the different sites, including the Weibull parameters, the AEP is calculated using Equation 6. The results of these calculations are organized in Table 5. This table also compares the increase in AEP achieved by the optimized and scaled turbine blades against the baseline blade.

The data presented in Table 5 indicate that the Tarhuna site has a higher energy yield than the Almqrun site, as expected due to its greater average wind speed. An additional finding is the impact of the optimized pitch on AEP: Tarhuna experiences a 13.87% increase compared to a 7.34% increase for Almqrun. This discrepancy arises because the optimized pitch results in a greater power output over the baseline blade, particularly at wind speeds exceeding 11 m/s. As Figure 4 illustrates, the power generation differential with optimized pitch becomes markedly noticeable beyond this speed threshold. The wind data underscores that only 3.8% of Almqrun's wind speeds surpass 11 m/s, while in Tarhuna, this figure is about 16%, making the optimized pitch especially beneficial for Tarhuna due to its higher incidence of strong winds.

For calculating the PVC, it's necessary to establish the values of various factors as delineated in Equation 7. This research determines these values based on certain assumptions that are commonly accepted in the literature [23, 24]. The calculated terms, assumptions made, and the resultant PVC are documented in Table 6. The cost estimation for the turbine, as referenced from Adaramola et al. [25], is $1775 per kW for commercial wind turbines with an approximate rated power of 20kW. It's noted that an additional 3% of the turbine's cost is accounted for in the baseline turbine to incorporate the pitch mechanism. Furthermore, it is posited that any increase in turbine size, as per a specific scale factor, would proportionately escalate the turbine's price.

The cost in U.S. cents /kWh produced by the wind turbine, is computed using Equation 8, assuming a turbine lifespan of 20 years. Table 7 details the resulting electricity costs, while Table 8 displays the cost reductions for electricity when comparing the optimized and differently scaled turbine blades to the baseline blade. These tables not only provide the cost figures but also illustrate the relative cost efficiency gains achieved by implementing the optimized pitch and scaling the turbine size.

The calculated costs represent the breakeven point for the wind turbine's electricity pricing, ensuring it can recoup its investment over the designated lifespan of 20 years. According to data from statistical websites, the global average electricity price falls between 8 to 15 cents per kWh. Given this, the Tarhuna site emerges as a viable location for wind energy endeavors, with the original turbine blade producing electricity at a cost of 4.36 cents per kWh, which is below the worldwide average. However, for the Almqrun site to become economically viable and bring the cost of electricity below the global average minimum, it would be necessary to implement an optimum pitch and scale the turbine blades by a factor of 1.15.

Table 5. AEP Comparison for different sites and configurations

Site	Baseline	Optimum Pitch		1.05 Scale Factor		1.10 Scale Factor		1.15 Scale Factor	
	AEP (MWh)	AEP (MWh)	Increase (%)	AEP (MWh)	Increase (%)	AEP (MWh)	Increase (%)	AEP (MWh)	Increase (%)
Almqrun	25.08	26.92	7.34	29.80	18.82	32.70	30.38	35.74	42.50
Tarhuna	53.28	60.67	13.87	66.72	25.23	72.83	36.69	79.09	48.44

Table 6. The computed PVC

Term	Assumed/Calculated Value				
	Baseline	**Optimum Pitch**	**1.05 Scale**	**1.10 Scale**	**1.15 Scale**
Turbine cost	35,145 USD	36,200 USD	38,000 USD	39,820 USD	41,630 USD
Investment, I	42,174 USD	43,440 USD	45,610 USD	47,780 USD	49,950 USD
OMR cost, $?_{???}$	440 USD	453 USD	475 USD	498 USD	520 USD
Inflation Rate, i	0.12	0.12	0.12	0.12	0.12
Interest Rate, r	0.15	0.15	0.15	0.15	0.15
Scrap Value, S	4,220 USD	4,345 USD	4,560 USD	4,780 USD	5,000 USD
PVC	46,420 USD	47,820 USD	50,200 USD	52,600 USD	55,000 USD

Table 7. Electricity cost

Site	Electricity cost (USD cent/kWh)				
	Baseline	**Optimum Pitch**	**1.05 Scale**	**1.10 Scale**	**1.15 Scale**
Almqrun	9.25	8.88	8.43	8.04	7.69
Tarhuna	4.36	3.94	3.76	3.61	3.48

Table 8. Reduction in electricity cost (%)

Site	Electricity cost reduction (%)			
	Optimum Pitch	**1.05 Scale**	**1.10 Scale**	**1.15 Scale**
Almqrun	4.05	8.96	13.11	16.89
Tarhuna	9.54	13.64	17.11	20.20

In addition to the discussed references, there are many other researches in literature regarding renewable energy and its applications such as in references [26-30].

7. Conclusion

The study integrates Computational Fluid Dynamics (CFD) analysis with wind resource assessment. CFD analysis was utilized to determine the optimal pitch angle at the blade tip across various wind speeds of stall-regulated wind turbine, which was then modified to a pitch-regulated turbine. This modified turbine was scaled to three different sizes to examine the impact of blade pitch angle and size adjustments on Annual Energy Production and the cost of generated electricity.

Findings indicate that converting to a pitch-regulated turbine and employing an optimal pitch angle at wind speeds below the nominal speed significantly improves the wind turbine performance. Specifically, the optimized configuration increases the power production by around of 8% for wind speeds up to 12 m/s, and remarkably by an by around 154% for wind speeds exceeding 12 m/s, when compared to the original wind turbine blade.

When combined with scaling factors, the power output with an optimized pitch shows additional increases by average percentages of 33.1 %, 21.7 % and 10.7%, for size scale factors of 1.15, 1.10 and 1.05 respectively. This suggests a pattern where a 5% increase in blade size correlates with an approximate 11% boost in power output. However, for a comprehensive validation of this size-to-power output relationship, further research is necessary across different wind turbines and a broader range of scales.

Based on those outcomes, the results demonstrate significant increases in AEP for both investigated sites, as well as notable reductions in electricity costs.

References

[1] M. Sessarego, N. Ramos-Garcia, H. Yang & W. Z. Shen, "Aerodynamic wind-turbine rotor design using surrogate modeling and three-dimensional viscous - inviscid interaction technique," Renew Energ. 2016, 93, 620-635, DOI: 10.1016/j.renene.2016.03.027.

[2] T. Dhert, T. Ashuri & J. R. R. A. Martins, "Aerodynamic shape optimization of wind turbine blades using a Reynolds-averaged Navier–Stokes model and an adjoint method," Wind Energy. 2016, 20, 909-926, DOI: 10.1002/we.2070.

[3] J. Sumner, C. S. Watters & C. Masson, "CFD in wind energy: The virtual, multiscale wind tunnel," Energies 2010, 3, 989-1013, DOI: 10.3390/en3050989.

[4] M. A. Elfarra, N. S. Uzol & I. S. Akmandor, "NREL VI rotor blade: numerical investigation and winglet design and optimization using CFD," Wind Energy 2013, 17, 605-626, DOI: 10.1002/we.1593.

[5] M. A. Elfarra, N. S. Uzol & I. S. Akmandor, "Investigations on blade tip tilting for HAWT rotor blades using CFD," Int J Green Energy 2015, 12, 125-138, DOI: 10.1080/15435075.2014.889007.

[6] T. D. Economon, F. Palacios & J. J. Alonso, "A viscous continuous adjoint approach for the design of rotating engineering applications," 21st AIAA Computational Fluid Dynamics Conference, AIAA Paper 2013, No: 2013-2580, DOI: 10.2514/6.2013-2580.

[7] A. Alaimo, A. Esposito, A. Milazzo, C. Orlando& F. Trentacosti, "Slotted blades savonius wind turbine analysis by CFD," Energies 2013, 6, 6335-6351, DOI:10.3390/en6126335.

[8] A. Alaimo, A. Esposito, A. Messineo, C. Orlando & D. Tumino, "3D CFD analysis of a vertical axis wind turbine," Energies 2015, 8, 3013-3033, DOI:10.3390/en8043013.

[9] B. Shahizare, N. N. Ghazali, W. T. Chong, S. S. Tabatabaeikia & N. Izadyar, "Investigation of the optimal omni-direction-guide-vane design for vertical axis wind turbines based on unsteady flow CFD simulation," Energies 2016, 9, 146, DOI: 10.3390/en9030146.

[10] J. Cao, W. Zhuy, T. Wangz & S. Kex, "Aerodynamic optimization of wind turbine rotor using CFD/AD method," Modern Physics Letters B 2018, 32, DOI: 10.1142/S0217984918400535.

[11] J. Cao, W. Zhu, W. Shen, J. N. Sørensen & T. Wang, "Development of a CFD-based wind turbine rotor optimization tool in considering wake effects," Appl. Sci. 2018, 8, 2056, DOI: 10.3390/app8071056.

[12] H. Jiang, J. Wang, Y. Dong & H. Lu, "Comprehensive assessment of wind resources and the low-carbon economy: an empirical study in the Alxa and Xilin Gol Leagues of inner Mongolia, China," Renew. Sustain. Energy Rev. 2015, 50, 1304-1319, DOI: 10.1016/j.rser.2015.05.082.

[13] M. Hand, D. Simms, L. Fingersh, D. Jager, J. Cotrell & S. Schreck. Larwood, "Unsteady Aerodynamics Experiment Phase VI: Wind Tunnel Test Configurations and Available Data Campaigns," National Renewable Energy Laboratory, NREL/TP 500-29955, Golden, CO, 2001.

[14] P. Giguere & M. S. Selig, "Design of a Tapered and Twisted Blade for the NREL Combined Experiment Rotor," National Renewable Energy Laboratory, NREL/SR-500-26173, Golden, CO, April 1999.

[15] N. Hakimi, "Preconditioning Methods For Time Dependent Navier-Stokes Equations," PhD Thesis 1997, Dept of Fluid Mechanics, Vrije Universiteit Brussel.

[16] A. S. Shata & R. Hanitsch, "The potential of electricity generation on the east coast of Red Sea in Egypt," Renew. Energy 2006, 3, 1597-1615, DOI: 10.1016/j.renene.2005.09.026.

[17] I. Y. F. Lun & L. C. A. Joseph, "A study of weibull parameters using long-term wind observations," Renew. Energy 2000, 20, 145–153, DOI: 10.1016/S0960-1481(99)00103-2.

[18] O. A. Jaramillo, R. Salana & U. Miranda, "Wind power potential of Baja California Sur, Mexico," Renew. Energy 2004, 29, 2087–2100, DOI: 10.1016/j.renene.2004.03.004.

[19] M. A. Elfarra & A. Silini, "Technical and economical evaluation and GHG analysis of wind power generation in four sites using different weibull parameters," International Journal of Renewable Energy Research, Vol.8, No.3, 2018. DOI: 10.20508/ijrer.v8i3.8082.g7471.

[20] M. A. Elfarra & M. Kaya, "Comparison of optimum spline-based probability density functions to parametric distributions for the wind speed data in terms of annual energy production," Energies, 2018. DOI:10.3390/en11113190

[21] A. D. Miguel & J. Bilbao, "Test reference year generation from meteorological and simulated solar

radiation data," Sol. Energy 2005, 78, 695- 703, DOI: 10.1016/j.solener.2004.09.015.

[22] F. Fazelpour, E. Markarian & N. Soltani, "Wind energy potential and economic assessment of four locations in Sistan and Balouchestan province in Iran," Renew. Energy 2017, 109, 646-667, DOI: 10.1016/j.renene.2017.03.072.

[23] A.S. Shata & R. Hanitsch, "Electricity generation and wind potential assessment at Hurghada, Egypt," Renew. Energy 2008, 33, 141-148, DOI: 10.1016/j.renene.2007.06.001.

[24] M. O. L. Hansen, "Aerodynamics of Wind Turbines," 2nd ed.; Earthscan: London, UK, 2008, pp. 55-57, 978-1-84407-438-9.

[25] M. S. Adaramola, S. S. Paul & S. O. Oyedepo, "Assessment of electricity generation and energy cost of wind energy conversion systems in north-central Nigeria," Energy Convers. Manag. 2011, 52 , 3363–3368, DOI: 10.1016/j.enconman.2011.07.007.

[26] A. B. Bayındır, A. Shraida, S. Bayhan, H. Abu-Rub, "Design and implementation of microcontroller based three phase induction motor experimental set," 10th International Conference on Smart Grid, June 27-29, 2022, Istanbul / Turkey.

[27] V. Matin, M. Ali, D. L. Donovin, F. E. John & M. I. Dan, "Coreless Axial Flux Halbach Array Permanent Magnet Generator Concept for Direct-Drive Wind Turbine," 12th International Conference on Renewable Energy Research and Applications, August 29 - September 1, 2023, Oshawa, Canada.

[28] M. Sakai & T. Takeshita, "Energy management system of electric motorcycles for power boost," 12th International Conference on Renewable Energy Research and Applications, August 29 - September 1, 2023, Oshawa, Canada.

[29] D. Nihat, U. Berat & B. Erdal, "Measurement and evaluation of solar panel data via DC power line," 10th International Conference on Smart Grid, June 27-29, 2022, Istanbul / Turkey

[30] S. Satoshi & S. Orie, "Voltage control of DFIG-based wind turbine generator in rural grid," 12th International Conference on Renewable Energy Research and Applications, August 29 - September 1, 2023, Oshawa, Canada.